AGU PUBLICATIONS

Journal of Advances in Modeling Earth Systems

RESEARCH ARTICLE

10.1002/2016MS000863

Improvement of the prediction of surface ozone concentration over conterminous U.S. by a computationally efficient second-order Rosenbrock solver in CAM4-Chem

Jian Sun[1], Joshua S. Fu[1,2], John Drake[1], Jean-Francois Lamarque[3], Simone Tilmes[3], and Francis Vitt[3]

[1]Department of Civil and Environmental Engineering, University of Tennessee, Knoxville, Tennessee, USA, [2]Climate Change Science Institute and Computer Science and Mathematics Division, Oak Ridge National Laboratory, Oak Ridge, Tennessee, USA, [3]National Center for Atmospheric Research, Boulder, Colorado, USA

Key Points:
- The second-order Rosenbrock solver significantly reduces the positive bias of surface ozone concentration over CONUS, Europe, and East Asia
- By refining the time step size, the first-order implicit solver used in CAM4-Chem fails to offer a statistically significant improvement
- The second-order Rosenbrock solver is almost twice as fast as the original first-order implicit solver

Correspondence to:
J. S. Fu,
jsfu@utk.edu

Citation:
Sun, J., J. S. Fu, J. Drake, J.-F. Lamarque, S. Tilmes, and F. Vitt (2017), Improvement of the prediction of surface ozone concentration over conterminous U.S. by a computationally efficient second-order Rosenbrock solver in CAM4-Chem, *J. Adv. Model. Earth Syst.*, *9*, doi:10.1002/2016MS000863.

Received 16 NOV 2016
Accepted 5 FEB 2017
Accepted article online 11 FEB 2017

Abstract The global chemistry-climate model (CAM4-Chem) overestimates the surface ozone concentration over the conterminous U.S. (CONUS). Reasons for this positive bias include emission, meteorology, chemical mechanism, and solver. In this study, we explore the last possibility by examining the sensitivity to the numerical methods for solving the chemistry equations. A second-order Rosenbrock (ROS-2) solver is implemented in CAM4-Chem to examine its influence on the surface ozone concentration and the computational performance of the chemistry program. Results show that under the same time step size (1800 s), statistically significant reduction of positive bias is achieved by the ROS-2 solver. The improvement is as large as 5.2 ppb in Eastern U.S. during summer season. The ROS-2 solver is shown to reduce the positive bias in Europe and Asia as well, indicating the lower surface ozone concentration over the CONUS predicted by the ROS-2 solver is not a trade-off consequence with increasing the ozone concentration at other global regions. In addition, by refining the time step size to 180 s, the first-order implicit solver does not provide statistically significant improvement of surface ozone concentration. It reveals that the better prediction from the ROS-2 solver is not only due to its accuracy but also due to its suitability for stiff chemistry equations. As an added benefit, the computation cost of the ROS-2 solver is almost half of first-order implicit solver. The improved computational efficiency of the ROS-2 solver is due to the reuse of the Jacobian matrix and lower upper (LU) factorization during its multistage calculation.

1. Introduction

Atmospheric chemistry is important for global climate simulation because of the close coupling of transport, physical, chemical, and biological processes. The feedbacks among chemical reactions, climate equilibria, anthropogenic emissions, and land use changes provide a new dynamical perspective on global and regional climate and air quality predictions. Among the atmospheric chemical constituents, tropospheric ozone is a critical pollutant that can significantly affect ecosystems, agriculture productions, public health, and climate forcing [*Stevenson et al.*, 1998; *Fiscus et al.*, 2005; *Karnosky et al.*, 2007; *Cooper et al.*, 2010; *Sun et al.*, 2015]. However, ozone is not directly emitted and its complex photochemical reaction mechanism makes its simulation a challenge. Significant bias in the prediction of ozone concentration exists zonally and seasonally for both single model output [*Zeng et al.*, 2008; *Lamarque et al.*, 2012; *Val Martin et al.*, 2015] and multimodel ensemble mean results [*Stevenson et al.*, 2006, 2013; *Young et al.*, 2013]. There are also inconsistencies between the estimated ozone concentration from global climate models and the observed seasonal cycle [*Fiore et al.*, 2014]. In the CAM4-Chem model we are using, optimizing the dry deposition scheme based on land use changes has significantly improved the simulation of summertime (June, July, and August, JJA) surface ozone concentration over the U.S. [*Val Martin et al.*, 2014, 2015]. However, further efforts are required to reduce the remaining bias.

Few studies have investigated the numerical chemical solver itself in the performance of global chemistry-climate models. *Shampine* [1982] studied initial value problems for stiff systems of ordinary differential equations (ODEs) and proposed an approach to automatically select either an explicit Runge-Kutta formula

or Rosenbrock formula at every time step. The Rosenbrock method was competitive with the backward differentiation formulas (BDF) in some circumstances. The sparse matrix vectorized gear code (SMVGEAR) developed by *Jacobson and Turco* [1994] was also implemented in global chemistry models such as GMI [*Rotman et al*., 2001], IMPACT [*Rotman et al*., 2004], GATOR-GCMOM [*Jacobson and Ginnebaugh*, 2010; *Jacobson et al*., 2015], and GEOS-Chem [*Zhang et al*., 2011]. However, this solver used an iterative method to solve the ODEs and included the reevaluation of the Jacobian matrix during the iteration, which was intrinsically slower than other solvers using a noniterative method. *Sandu et al*. [1997] tested a set of box-model atmospheric chemistry problems (TMK model, CBM-IV model, AL model, a NASA HSRP/AESA stratospheric model, and an aqueous model) with different solvers, including LSODE (Livermore Solver for Ordinary Differential Equations) and Variable-coefficient Ordinary Differential Equation solver (VODE) that were expected to perform similarly to SMVGEAR. The benchmark problems covered a wide range of photolytic, homogeneous (gas phase, liquid phase) and heterogeneous (gas-liquid) reactions. The results showed that the Rosenbrock solvers were the most cost effective and performed well for real problems with large variety of conditions that could occur at different grid cells. *Verwer et al*. [1999] applied a second-order, L-stable Rosenbrock (ROS-2) method to the three-dimension atmospheric reaction and transport problem including photochemistry, advection, and diffusion. Three chemistry models (RIVM, CBM-IV, and WET) using the ROS-2 method were examined and the ROS-2 method was proven to be an excellent candidate for global air quality modeling with large time steps on the order of minutes. *Blom and Verwer* [2000] examined different operator-splitting methods for the atmospheric transport-chemistry problems and the test results revealed that the Rosenbrock W-method, split at the linear algebra level, was a better option than Strang operator-splitting or source splitting. The W-method avoided the artificial stiff transients during the chemistry computation and boundary condition issues for integration in time, though its implementation was complex. *Long et al*. [2013] developed a coupled chemistry and climate system model by linking the NCAR Community Atmosphere Model (modal-CAM v3.6.33, the atmospheric component of Community Climate System Model (CCSM3)) and the Max Planck Institute for Chemistry's Module Efficiently Calculating the Chemistry of the Atmosphere (MECCA; v2.5) to investigate the multiphase process in the atmosphere. The Kinetics PreProcessor (KPP) [*Sandu and Sander*, 2006] package was used to provide user-defined solvers and the benchmark intercomparison among three solvers from the Rosenbrock family, namely ROS-2, ROS-3, and RODAS-3, showed good agreement for ozone and OH radical prediction. Note that only the atmospheric component was considered in the work of *Long et al*. [2013] and the effect of different solvers in a long-term simulation was not explored.

In this paper, we do not achieve improvement by a better design of the sparse matrix. Breaking the data structure in order to introduce some external packages would disable existing optimizations. Instead, we seek to obtain improved performance of chemistry and computation from the algorithm itself. Therefore, based on the literature above, the numerical solvers from the Rosenbrock family are good alternatives for full atmospheric chemistry and climate simulation. These methods have already been incorporated into some regional models such as the Weather Research and Forecasting model coupled with Chemistry (WRF-Chem) and the Community Multi-scale Air Quality Model (CMAQ) [*Linford et al*., 2009; *Sarwar et al*., 2013]. But their use in global models is very limited. In this study, the global climate model we use is the Community Earth System Model (CESM) with online chemistry activated (CAM4-Chem) [*Lamarque et al*., 2012]. Currently the chemical solver uses a fully implicit Euler method that gives unconditional stability but only first-order accuracy in time [*Kinnison et al*., 2007]. This could be part of the reason for poor performance of ozone in previous work with CAM4-Chem. To bridge the gap between the need for better estimate of ozone from a scientific perspective and the limitation of a low order accuracy solver in the current CAM4-Chem, the ROS-2 solver is implemented to replace the original chemical solver and tested to see whether there is any benefit for the global climate and chemistry simulation. Unlike the implicit Euler method, the ROS-2 method avoids the reevaluation and redecomposition of the Jacobian matrix. These are the most time-consuming parts in a chemical solver [*Daescu et al*., 2000]. Hence, we are also interested in the improvement of computational performance of chemistry with the ROS-2 solver. The mathematical formula of the ROS-2 method and its implementation in CAM4-Chem are described in the methodology section. The predictions of surface ozone concentration over the conterminous U.S. (CONUS) between the ROS-2 solver and the original first-order implicit solver are compared, as well as their computational efficiencies with varying numbers of processors on a massively parallel supercomputer. Finally, we discuss the major differences we have observed, and make further recommendations.

2. Methodology

2.1. Chemistry Configuration in CAM4-Chem

The Community Earth System Model (CESM version 1.2.2) is a state-of-the-art global climate model. It consists of four components: atmosphere, land and land-ice, ocean, and sea ice. CAM4-Chem is an implementation of atmospheric chemistry in CESM and its chemistry is fully coupled with the radiative absorption processes of the Community Atmosphere Model, the atmospheric component of CESM (CAM4) [*Neale et al*., 2013]. The chemistry mechanism in the current CAM4-Chem version is adapted from the standard Tropospheric Model for Ozone and Related chemical Tracers (MOZART-4) [*Emmons et al*., 2010]. However, more chemistry-specific parameterization such as dry/wet deposition schemes and species types are expanded in the current CAM4-Chem version. The details about their differences, together with CAM4-Chem's representation of atmospheric chemistry in the global model, are well evaluated in previous work [*Lamarque et al*., 2012]. In total, the chemical mechanism includes 212 reactions, with 40 photochemical reactions and 172 gas phase reactions. There are 103 chemical species: 8 species (CH_4, N_2O, CO, Rn, Pb, H_2, HCN, and CH_3CN) are solved explicitly by the first-order (forward) Euler method and the remaining 95 species are solved implicitly by a backward Euler method with a Newton-Raphson iteration for quick convergence. These 95 species include all the chemically active species such as ozone and OH radicals, which contribute most to the stiffness of the system. In this study the ROS-2 solver will be developed to replace the implicit solver mentioned above. The finite-volume (FV) dynamical core [*Neale et al*., 2010] is used with a global horizontal resolution of 0.9° (latitude) by 1.25° (longitude) and 26 vertical layers top to approximately 3 hPa.

2.2. ROS-2 Solver Description

In the state-of-the-art CAM4-Chem version, an operator-splitting approach is used and the atmospheric chemical reactions are integrated by the stiff ODE solver separately from other processes like dynamics and physics. Thus, for the chemistry update, each control volume behaves like a box model. The equations for chemical species conservation and reaction in the atmosphere take the form of an autonomous system:

$$\frac{Dy}{Dt} = F(y) = P(y) - L(y) + I(y) \tag{1}$$

where $y = (y_1, y_2, \ldots, y_N)^T$ is the vector of volume mixing ratios for N species (N here represents the 95 implicit species) at given latitude, longitude, and vertical coordinate; the source term F(y) represents the atmospheric chemical reactions. It can be further decomposed into three components: production P(y), loss L(y), and independent forcing I(y) terms. P(y) and L(y) are mainly calculated by the species mixing ratios and reaction rates, while I(y) is evaluated based on the external forcing (i.e., aircraft and lightning emissions). The two-stage, linear-implicit Rosenbrock scheme for the ODE above can be written as *Verwer et al*. [1999]:

$$(I - h\gamma A)k_1 = F(y^n) \tag{2}$$

$$(I - h\gamma A)k_2 = F(y^n + hk_1) - 2k_1 \tag{3}$$

$$y^{n+1} = y^n + \frac{3}{2}hk_1 + \frac{1}{2}hk_2 \tag{4}$$

where I is an N × N identity matrix; h is the time step size; $A = \frac{\partial F(y)}{\partial y}|_{y=y^n}$ is the Jacobian matrix at time $t = t^n$; y^n and y^{n+1} are the solution vectors of species mixing ratios at time $t = t^n$ and t^{n+1}, respectively. Vectors k_1 and k_2 are the intermediate solutions at each stage. Parameter γ is a constant and appears in the stability function with $z = h\alpha$ for problem $y' = \alpha y$ as

$$R(z) = \frac{1 + (1 - 2\gamma)z + \left(\frac{1}{2} - 2\gamma + \gamma^2\right)z^2}{(1 - \gamma z)^2} \tag{5}$$

A solver is defined as A-stable if $|R(z)| \leq 1$ as $z \to \infty$ and it is further called L-stable if $R(z) \to 0$ as $z \to \infty$. The ROS-2 solver proposed above is A-stable for equation (5) if and only if $\gamma \geq \frac{1}{4}$. Furthermore, by choosing $\gamma = 1 \pm \frac{1}{\sqrt{2}}$ this scheme becomes L-stable ($R(\infty) = 0$), which is good for simulating some chemical species with a short life span in the atmosphere. In practice, $\gamma = 1 + \frac{1}{\sqrt{2}}$ is usually chosen due to its better nonlinear stability behavior under large time steps [*Verwer et al*., 1999] and this value is thus used in this study. An obvious advantage to the implementation of the ROS-2 solver is that it does not require the reevaluation of the Jacobian matrix at each stage, while the Newton method requires the reevaluation of the Jacobian

matrix during each iteration. Therefore, it can utilize the same "lower upper" (LU) factorization result at each stage of the solution update. Since updating the Jacobian matrix and conducting the LU factorization are the most time-consuming operation, this benefit should speed up the chemistry update and save much computation time [*Daescu et al*., 2000].

2.3. Time Step Size Setting

In this work, h = 180 and 1800 s are chosen as two different time step sizes to examine whether the first-order implicit solver and the ROS-2 solver can benefit from the time refinement. It is noted that the previous literature claimed that the ROS-2 solver was able to work under time step size of 600 and 900 s [*Verwer et al*., 1999; *Blom and Verwer*, 2000]. However, those studies were either working on a simple chemical mechanism or a benchmark simulation without considering the complexity of an earth system model. Furthermore, they agreed that the necessity to form a better conditioned system, resolve the initial transients accurately and handle the nonlinear chemistry in the real atmosphere might require a more restricted time step size [*Shampine*, 1982; *Sandu et al*., 1997; *Verwer et al*., 1999; *Blom and Verwer*, 2000]. In addition, the concepts of A-stability and L-stability are defined for an idealized linear system. The real atmospheric chemistry system is nonlinear and can be very stiff with the existence of fast and slow reacting species. Thus, a small time step is usually recommended to make the chemical reaction system valid for "linearization" (keep the property of linear system) and avoid impacting the quality of numerical integration. Based on those concerns, we implement an adaptive time step method for the ROS-2 solver when the time step size equals 1800 s. If the program detects a location where a negative solution is generated by the ROS-2 solver, it refines the time step by a factor of 2 for that location and recomputes the chemistry. This procedure is repeated until the refined time step size is less than 180 s, in which case we simply set the time step size to 180 s to save computation time. We have found that the ROS-2 solver can run continuously with a fixed 180 s time step for the standard full tropospheric chemistry mechanism TROP_MOZART [*Emmons et al*., 2010].

2.4. Algorithm and Implementation

The steps of the algorithm are as follows:

a. Calculate the independent forcing term, which is treated as invariant as in the original first-order implicit solver design.
b. Calculate the linear and nonlinear components of Jacobian matrix to form the left-hand side system in equations (2) and (3). CAM4-Chem uses the same chemical preprocessor as MOZART-4 [*Lamarque et al*., 2012], which reads the specific chemical mechanism file and converts it into Fortran code to provide the input for the calculation of linear and nonlinear parts. For the TROP_MOZART mechanism, there are 737 nonzero matrix entries of the system matrix and they are computed explicitly and exactly. The sparsity pattern reveals a classic "arrow matrix" ordering with the arrow pointing up as shown in Figure 1a. If the LU factorization is performed directly on this matrix, almost all the entries in the upper right matrix will be changed from an initial zero to a nonzero value during the execution. This is known as a fill-in issue [*Lee*, 2010] and it will significantly increase the cost of computation, which is determined by the total number of nonzero entries rather than by the size of the sparse matrix. Therefore, a permutation operator is applied before doing the LU factorization and the system matrix is flipped over to point down (see Figure 1b). The LU factorization starts with the nearly diagonal part of the matrix and all fill-ins occur down the right-hand side column where there are already a lot of nonzero entries. Note that although the system is different between the first-order implicit solver and the ROS-2 solver, the formation of the Jacobian matrix is exactly the same. Hence, the routines from the original first-order implicit solver can be used directly with only minor modification. It is also worth noting that in other solvers like SMVGEAR, the JSPARSE algorithm developed by *Jacobson and Turco* [1994] is used to reorder the Jacobian matrix based on the combined production and loss terms. In addition, the partial pivoting process is removed from the decomposition process to further reduce the number of matrix calculation. Instead, the chemical preprocessor of CAM4-Chem uses a diagonal Markowitz scheme [*Lee*, 2010] to reorder the Jacobian matrix, which searches on diagonal elements and chooses the pivot with the smallest Markowitz weight.
c. Form the LU factorization for the system matrix. As shown in Figure 1, the system matrix is very sparse with about 90% zeroes. In the current version of CAM4-Chem, the LU factorization is hardwired with a fixed pivoting order by knowing exactly the nonzeroes of system matrix. There are a total of 824 nonzero

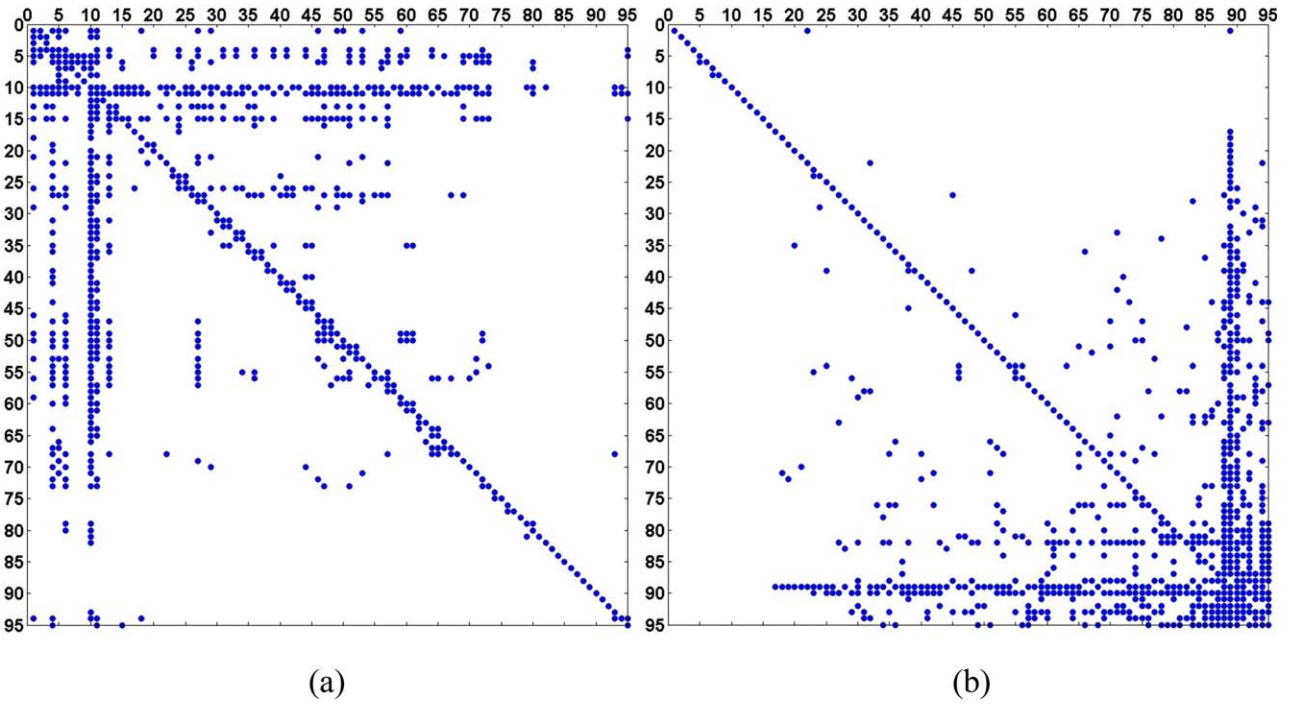

Figure 1. The sparsity pattern of left-hand side system matrix from the second-order Rosenbrock method (ROS-2) for the TROP_MOZART mechanism (a) before and (b) after permutation.

matrix entries after performing the LU factorization. Since the hardwired LU factorization does not need to test for pivots, the routine is highly optimized and efficient. It should be mentioned that extensive testing is done to ensure that the pivot strategy is robust even with the modification of the system in the ROS-2 formulas. We compared the accuracy of LU solution by capturing selected system matrices (examples used in section 3.1) and analyzing them in MATLAB. The results showed that either full pivoting (including both row and column pivoting) or partial pivoting (only including row pivoting) had no appreciable impact on the accuracy of solution as compared with the fixed pivoting strategy.

d. Calculate the source term F on the right-hand side.
e. Solve for the first-stage solution vector k_1 with explicitly programmed steps of reduction.
f. Update source term F for the second stage with intermediate approximation $y^n + hk_1$.
g. Solve for the second-stage solution vector k_2 using the same LU factorization result from the first stage.
h. Update species mixing ratio vector from y^n to y^{n+1} for the next time step.

3. Results and Discussion

3.1. Numerical Analysis of the First-Order Implicit Solver and the ROS-2 Solver

Before comparing the model simulation results, it is necessary to verify that both solvers converge to the same solution if the time step is small enough and they provide the numerical convergence rate as we expect. In order to verify this, a test problem is chosen for a linear system $\frac{du}{dt} = u$. Given the initial condition $u_0 = 1$ at $t_0 = 0$, it is trivial to derive the analytical solution, $u(t) = e^t$. By arbitrarily setting $t_{end} = 2$, separate numerical simulations with different time step sizes are performed to integrate from t_0 to t_{end} and the numerical results for both solvers are summarized in Table 1. Note that for the ROS-2 solver, we only use the given fixed time step size for verification tests and no refinement of time step is involved. In Table 1, Δt is the time step size for a numerical simulation; Abs (Error1) is the absolute error between the exact solution and the numerical solution generated by the first-order implicit solver at time $= t_{end}$; Rate1 is the ratio of current absolute error over the previous absolute error with twice time step size for the first-order implicit solver; Abs (Error2) and Rate2 are the same but for the numerical solution generated by the ROS-2 solver. The decimal precision of numerical results is shown as six digits so that the absolute error less than 1.E-06 is not included in the table. For the time step sizes finer than 1.25E-02, the error between exact solution and the

Table 1. Numerical Analysis of the First-Order Implicit Solver and Second-Order Rosenbrock (ROS-2) Solver for a Linear System

Δt	Abs(Error1)	Rate1	Abs(Error2)	Rate2
2.00E-01	1.924170E+00		1.580427E+00	
1.00E-01	8.362072E-01	0.434581	2.806979E-01	0.177609
5.00E-02	3.923089E-01	0.469153	5.946621E-02	0.211851
2.50E-02	1.902726E-01	0.485007	1.372136E-02	0.230742
1.25E-02	9.372968E-02	0.492607	3.297921E-03	0.240349
6.25E-03	4.652076E-02	0.496329	8.085571E-04	0.245172
3.13E-03	2.317529E-02	0.498171	2.001870E-04	0.247585
1.56E-03	1.156648E-02	0.499087	4.980504E-05	0.248793
7.81E-04	5.777966E-03	0.499544	1.242119E-05	0.249396
3.91E-04	2.887666E-03	0.499772	3.101549E-06	0.249698
1.95E-04	1.443504E-03	0.499886		
9.77E-05	7.216697E-04	0.499943		
4.88E-05	3.608143E-04	0.499972		
2.44E-05	1.804020E-04	0.499986		
1.22E-05	9.019972E-05	0.499993		
6.10E-06	4.509954E-05	0.499996		
3.05E-06	2.254969E-05	0.499998		
1.53E-06	1.127483E-05	0.499999		
7.63E-07	5.637408E-06	0.500000		
3.81E-07	2.818702E-06	0.500000		
1.91E-07	1.409351E-06	0.500000		

numerical solution generated by the first-order implicit solver is cut by half when the time step size is reduced by a factor of two, indicating a linear convergence of the first-order implicit solver and thus first-order numerical accuracy. On the other hand, a quadratic convergence (second-order accuracy) is observed for the ROS-2 solver as the error between exact solution and the numerical solution generated by the ROS-2 solver is cut by four when the time step size is reduced by a factor of two. Therefore, for a linear system, it proves that the convergence rate and accuracy of both solvers behave as we expect. Due to the quicker convergence of the ROS-2 solver, its absolute error with time step size equal to 3.91E-04 is already around 3.10E-06, while the absolute error for the first-order implicit solver with the same time step size is about 2.89E-03. However, Table 1 reveals that both solvers will eventually converge to the same solution as long as the time step size is small enough.

For the nonlinear system, the CAM4-Chem chemistry modules are first isolated such that other processes like dynamics and physics are excluded and the update of chemistry behaves exactly like a box model. Then input from some arbitrarily selected grid cells are used to provide the species concentrations, chemical reaction rates, and independent forcings as initial condition. Lastly, a series of box-model simulations are performed for one climate time step (1800 s by default) with different numerical time step sizes. We have tested input from different grid cells and they generally provide consistent results of numerical analysis. Hence, one grid at Eastern U.S. (latitude = 34.4°, longitude = −90.0°, level = 26 (bottom layer)) is used as an example for illustration (see Table 2a). Compared to Table 1, one additional column named "Ozone" is added to show the ozone concentration (units: mol/mol) from the box-model simulation after one climate time step. Note that the chemistry used in CAM4-Chem is a nonlinear system and therefore no analytical solution exists. A common approach to obtain the "exact" solution in this case is to solve the system with a very tiny numerical time step size. We find out that for the ROS-2 solver, when the time step size is about 1.76 s, the ratio of absolute difference between ozone solution calculated by 1.76 s and ozone solution calculated by 3.52 s over the ozone solution calculated by 3.52 s is smaller than 1.E-12, which is beyond the decimal precision in CAM4-Chem. Hence, 6.034342167442E-13 mol/mol is chosen as the "exact" solution here for numerical analysis. It turns out that the first-order implicit solver still converges linearly for this nonlinear system while a quadratic convergence is again observed for the ROS-2 solver. Table 2a also shows that if the time step size is small enough, the first-order implicit solver will still converge to the "exact" solution with relative error ("Abs(Error2)" column divided by "Ozone" column) smaller than 1.E-12. However, the ROS-2 solver behaves better here since the ROS-2 solver using a numerical time step size equal to 1800 s produces a solution with relative error smaller than 1.E-7.

It is worth noting that the initial condition for the convergence test above is from the initial data of CAM4-Chem. The species concentration (e.g., ozone) is a little away from the realistic chemistry state of the

Table 2. Numerical Analysis of the First-Order Implicit Solver and Second-Order Rosenbrock (ROS-2) Solver for a Nonlinear System With Box-Model Simulations (Units: mol/mol)

Δt	Ozone	Abs(Error)	Rate
(a) Input From Initial Data for CAM4-Chem			
First-Order Implicit Solver			
1.80E+03	6.033875081040E-13	4.670864013899E-17	
9.00E+02	6.034108571651E-13	2.335957908294E-17	0.500113
4.50E+02	6.034225356959E-13	1.168104830493E-17	0.500054
2.25E+02	6.034283759124E-13	5.840831817003E-18	0.500026
1.13E+02	6.034312962523E-13	2.920491926016E-18	0.500013
5.63E+01	6.034327564793E-13	1.460264834934E-18	0.500006
2.81E+01	6.034334866071E-13	7.301370989840E-19	0.500003
1.41E+01	6.034338516745E-13	3.650696949433E-19	0.500002
7.03E+00	6.034340342091E-13	1.825351129328E-19	0.500001
3.52E+00	6.034341254766E-13	9.126759599780E-20	0.500000
1.76E+00	6.034341711104E-13	4.563378492274E-20	0.500000
8.79E-01	6.034341939273E-13	2.281686398665E-20	0.499999
4.39E-01	6.034342053358E-13	1.140840099425E-20	0.499999
2.20E-01	6.034342110400E-13	5.704177929390E-21	0.499998
1.10E-01	6.034342138921E-13	2.852068971804E-21	0.499996
5.49E-02	6.034342153182E-13	1.425979000582E-21	0.499981
2.75E-02	6.034342160312E-13	7.129810184583E-22	0.499994
1.37E-02	6.034342163877E-13	3.564590052800E-22	0.499956
6.87E-03	6.034342165661E-13	1.780309368838E-22	0.499443
3.43E-03	6.034342166553E-13	8.885597969955E-23	0.499104
1.72E-03	6.034342166987E-13	4.546201610256E-23	0.511637
8.58E-04	6.034342167198E-13	2.442293167725E-23	0.537216
4.29E-04	6.034342167270E-13	1.716399771048E-23	0.702782
2.15E-04	6.034342167344E-13	9.780966456978E-24	0.569854
1.07E-04	6.034342167385E-13	5.651929639532E-24	0.577850
5.36E-05	6.034342167414E-13	2.744983514679E-24	0.485672
2.68E-05	6.034342167436E-13	5.820152649848E-25	0.212029
ROS-2 Solver			
1.80E+03	6.034341703907E-13	4.635350394929E-20	
9.00E+02	6.034342027413E-13	1.400284692707E-20	0.302088
4.50E+02	6.034342129412E-13	3.802968924664E-21	0.271585
2.25E+02	6.034342157557E-13	9.885179905049E-22	0.259933
1.13E+02	6.034342164924E-13	2.518129837532E-22	0.254738
5.63E+01	6.034342166807E-13	6.349792599436E-23	0.252163
2.81E+01	6.034342167283E-13	1.590192123632E-23	0.250432
1.41E+01	6.034342167402E-13	3.937993638863E-24	0.247643
7.03E+00	6.034342167432E-13	9.399687893379E-25	0.238692
3.52E+00	6.034342167440E-13	1.899324624283E-25	0.202063
1.76E+00	6.034342167442E-13		
(b) Input From CAM4-Chem Output After 3 Month Simulation			
First-Order Implicit Solver			
1.80E+03	5.978245102732E-08	4.756396646170E-11	
9.00E+02	5.976140850864E-08	2.652144778010E-11	0.557595
4.50E+02	5.975076715046E-08	1.588008960000E-11	0.598764
2.25E+02	5.974356744260E-08	8.680381741498E-12	0.546620
1.13E+02	5.973906259478E-08	4.175533919096E-12	0.481031
5.63E+01	5.973668923211E-08	1.802171253901E-12	0.431603
2.81E+01	5.973561178778E-08	7.247269202004E-13	0.402141
1.41E+01	5.973517535312E-08	2.882922579047E-13	0.397794
7.03E+00	5.973500657783E-08	1.195169678004E-13	0.414569
3.52E+00	5.973493966948E-08	5.260862329855E-14	0.440177
1.76E+00	5.973491143495E-08	2.437409320730E-14	0.463310
8.79E-01	5.973489874541E-08	1.168454599514E-14	0.479384
4.39E-01	5.973489277449E-08	5.713632806852E-15	0.488991
2.20E-01	5.973488988499E-08	2.824131301198E-15	0.494279
1.10E-01	5.973488846466E-08	1.403796901733E-15	0.497072
5.49E-02	5.973488776067E-08	6.998111962483E-16	0.498513
2.75E-02	5.973488741024E-08	3.493800075629E-16	0.499249
1.37E-02	5.973488723541E-08	1.745559012606E-16	0.499616
6.87E-03	5.973488714810E-08	8.723879520881E-17	0.499776
3.43E-03	5.973488710448E-08	4.361949686608E-17	0.500001
1.72E-03	5.973488708267E-08	2.180870287674E-17	0.499976
8.58E-04	5.973488707195E-08	1.109250524923E-17	0.508627
4.29E-04	5.973488706696E-08	6.096307879626E-18	0.549588
2.15E-04	5.973488706502E-08	4.160096441321E-18	0.682396
1.07E-04	5.973488706356E-08	2.696807320270E-18	0.648256

Table 2. (continued)

Δt	Ozone	Abs(Error)	Rate
ROS-2 Solver			
1.80E+03	5.958452613181E-08	1.503609290504E-10	
9.00E+02	5.968294173170E-08	5.194532915820E-11	0.345471
4.50E+02	5.971188939336E-08	2.299766750360E-11	0.442728
2.25E+02	5.972455856641E-08	1.032849445230E-11	0.449111
1.13E+02	5.973019079380E-08	4.696267055103E-12	0.454690
5.63E+01	5.973286765394E-08	2.019406917293E-12	0.430003
2.81E+01	5.973413490840E-08	7.521524604925E-13	0.372462
1.41E+01	5.973465434590E-08	2.327149588001E-13	0.309399
7.03E+00	5.973482583434E-08	6.122652349968E-14	0.263097
3.52E+00	5.973487236949E-08	1.469137010049E-14	0.239951
1.76E+00	5.973488354320E-08	3.517655699798E-15	0.239437
8.79E-01	5.973488616374E-08	8.971160996013E-16	0.255032
4.39E-01	5.973488682017E-08	2.406849016532E-16	0.268287
2.20E-01	5.973488699653E-08	6.432889656107E-17	0.267274
1.10E-01	5.973488704421E-08	1.664560031187E-17	0.258758
5.49E-02	5.973488705667E-08	4.190801385659E-18	0.251766
2.75E-02	5.973488705982E-08	1.043994577271E-18	0.249116
1.37E-02	5.973488706060E-08	2.619978784976E-19	0.250957
6.87E-03	5.973488706078E-08	7.629913970189E-20	0.291220
3.43E-03	5.973488706086E-08		

atmosphere due to the spin-up effect. Therefore, we further examine another case with the initial condition from the output of CAM4-Chem after 3 month simulation. It turns out that when the time step size is refined to 3.43E-3 s, the relative error of the ROS-2 solver is smaller than 1.E-12 and thus 5.973488706086E-08 mol/mol can be used as the "exact" solution for ozone (see Table 2b). For the ROS-2 solver, quadratic convergence is observed after the time step size is refined to 7.03 s and smaller, while the first-order implicit solver converges linearly at the similar scale. The first-order implicit solver at time step size equal to 1800 s surprisingly shows smaller relative error (7.95E-4) than that for the ROS-2 solver at the time step size equal to 1800 s (2.52E-3). However, both relative errors can be thought small enough when doing the analysis of ozone concentration in the realistic atmosphere. Overall, based on the box-model analysis here, it seems appropriate to use the ROS-2 solver with 1800 s time step for the real simulation of atmospheric chemistry.

3.2. First-Order Implicit Solver and ROS-2 Solver at 1800 s Time Step

We focus our analysis on annual and summertime mean surface ozone concentrations generated from a decadal simulation from 2001 to 2010. Using the 1800 s time step, the output from the ROS-2 solver (ROS-2_1800s) and the first-order implicit solver (ORI_1800s) are compared. Figure 2a shows a nationwide decrease of 10 year averaged annual mean surface ozone concentration between the ROS-2_1800s and the ORI_1800s (ROS-2_1800s minus ORI_1800s). The largest and smallest differences are −3.12 and −0.58 ppb at the grid-cell level. By averaging the whole corresponding grids inside each state, the state-level differences are summarized in Table 3 and the Student's *t* test suggests that the state-level differences of annual mean surface ozone concentration between the ROS-2_1800s and the ORI_1800s are statistically significant at α=0.05 for 47 states except Washington. Considering the 10 year averaged surface ozone concentration during the summer season when the photolytic reaction is the most active during the year, Figure 2b clearly presents an even larger difference than the annual difference, especially over the Northeastern U.S. The largest and smallest differences at the grid-cell level are −5.62 and −0.18 ppb, respectively. For the state level, the ROS-2_1800s again shows a lower prediction of summertime mean ozone concentration over the CONUS than the ORI_1800s, similar to that for the annual mean ozone concentration. According to Table 3, the Student's *t* test suggests that the differences are statistically significant over 42 out of 48 conterminous states at α=0.05, ranging from −5.17 to −0.75 ppb. We further evaluate both model results with the ground-level observation data obtained from the Air Quality System (AQS) archived by U.S. EPA (https://www.epa.gov/aqs, ∼1200 observation sites over the CONUS). For the difference of 10 year averaged annual mean surface ozone concentration between model and monitor data, Figures 3a and 3b show that both ORI_1800s and ROS-2_1800s are likely to produce more than 20 ppb overestimate at the Eastern and Western U.S. coastal areas. The ROS-2_1800s reduces the bias mainly over the Eastern U.S., consistent with the

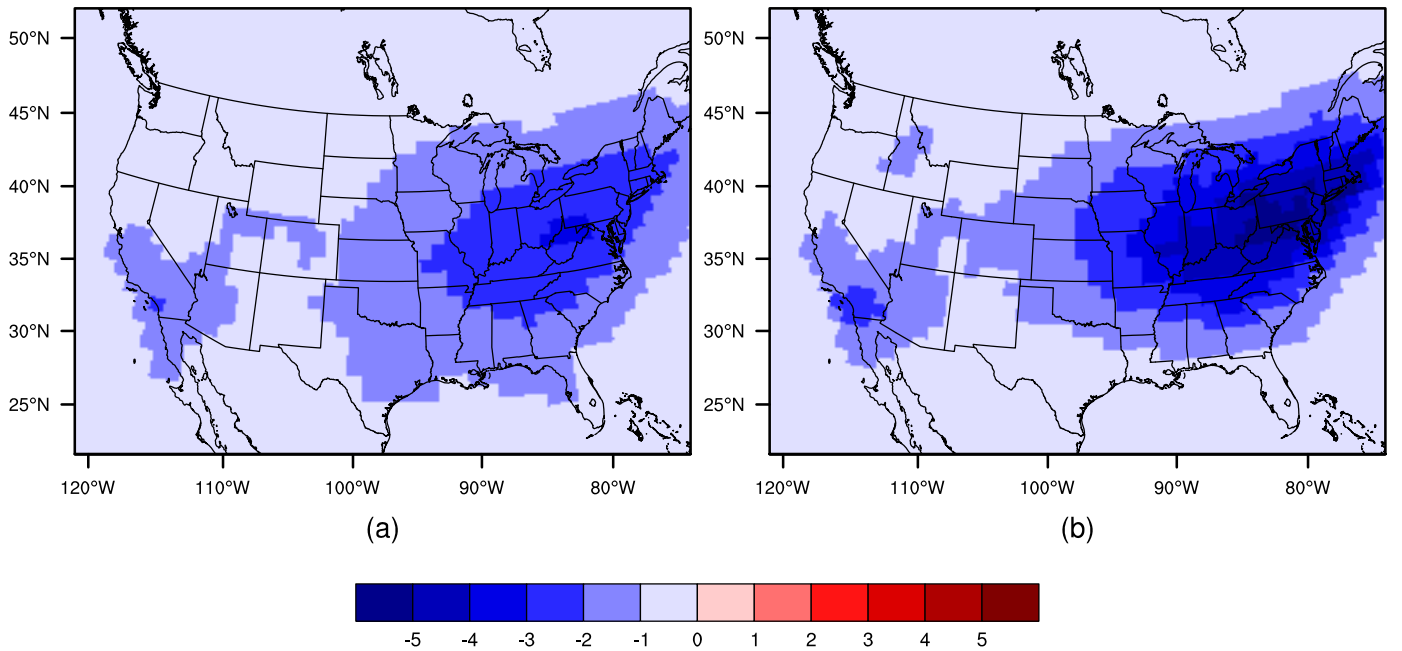

Figure 2. Difference of 10 year averaged (a) annual and (b) summertime (June, July, and August, JJA) mean surface ozone concentration (units: ppb) over the conterminous U.S. (CONUS) between the ROS-2 solver (ROS-2_1800s) and the first-order implicit solver (ORI_1800s) at 1800 s time step (ROS-2_1800s minus ORI_1800s).

plot in Figure 2a. The differences of 10 year averaged summertime mean surface ozone concentration between both solvers and AQS observation data are depicted in Figures 3c and 3d. The bias is even higher and could be larger than 30 ppb, especially over the Central (e.g., West Virginia) and Northeast (e.g., Pennsylvania). The overestimate of ozone concentration in the Eastern U.S. is a well-known issue from the previous literature about global chemistry-climate models [*Murazaki and Hess*, 2006; *Reidmiller et al.*, 2009; *Lapina et al.*, 2014], and potential reasons include coarse global resolution that fails to represent the steep topographic gradients in mixing depths [*Fiore et al.*, 2009] and disproportionate sensitivity of models at the high ozone concentration level [*Hollaway et al.*, 2012]. The spatial distribution of surface ozone concentration for the ROS-2_1800s presents an evident reduction of ozone bias at Southeast (e.g., Georgia), Central (e.g., Illinois), and Northeast (e.g., Pennsylvania). In addition, recalling the results of Student's *t* test, most of these reductions are statistically significant at $\alpha=0.05$. This reveals that the ROS-2_1800s is likely to significantly reduce the overestimate of surface ozone concentration to some extent, especially during the summer season.

3.3. First-Order Implicit Solver With 180 and 1800 s Time Step

Since a bias of surface ozone concentration is observed between the ORI-1800s and AQS monitor data, it is worth investigating whether refining the time step size is able to reduce the bias for the first-order implicit solver. The time step size in this study is refined to 180 s and the output from first-order implicit solver (ORI_180s) is compared with that from the ORI_1800s. Figure 4a shows a nationwide decrease of 10 year averaged annual mean surface ozone concentration between the ORI_180s and the ORI_1800s (ORI_180s minus ORI_1800s). The largest and smallest differences at the grid-cell level are -0.53 and -0.05 ppb, respectively. The state-level differences are listed in Table 4 and the mean normalized gross error E_{MNGE} is also calculated based on equation (6):

$$\text{Mean normalized gross error } E_{MNGE}=\frac{1}{N}\sum_{i=1}^{N}\left(\frac{|M_i-O_i|}{O_i}\right)\times 100\% \tag{6}$$

where N is the number of observations from AQS by time and space in each state; O_i and M_i are the ith values of observation and model in each state, respectively. Albeit the ORI_180s gives a widely lower estimate of surface ozone concentration and E_{MNGE}, the Student's *t* test shown in Table 4 suggests that the state-level differences of annual mean surface ozone concentration over the CONUS between the ORI_180s and the ORI_1800s are not statistically significant at $\alpha=0.05$. Considering the 10 year averaged summertime mean surface ozone concentration, Figure 4b presents that both positive and negative differences between

Table 3. Student's *t* Test for Difference (ROS-2_1800s Minus ORI_1800s, Units: ppb) Between the Second-Order Rosenbrock Solver (ROS-2-1800s) and the First-Order Implicit Solver (ORI-1800s) at 1800 s Time Step in Each State

State	Annual Mean Bias	*p* Value	Summertime Mean Bias	*p* Value
AL	−1.74	<0.001	−1.73	0.007
AZ	−1.10	<0.001	−1.32	<0.001
AR	−1.78	<0.001	−2.02	<0.001
CA	−1.20	<0.001	−1.28	0.044
CO	−0.99	<0.001	−1.09	<0.001
CT	−2.66	0.001	−4.84	<0.001
DE	−2.67	0.003	−4.63	<0.001
FL	−1.01	0.021	−0.62	0.400
GA	−1.67	<0.001	−1.79	0.035
ID	−0.76	0.008	−0.90	0.005
IL	−2.32	<0.001	−3.63	<0.001
IN	−2.60	<0.001	−4.20	<0.001
IA	−1.61	<0.001	−2.52	<0.001
KS	−1.27	<0.001	−1.66	<0.001
KY	−2.78	<0.001	−4.21	<0.001
LA	−1.24	0.002	−0.72	0.348
ME	−1.49	<0.001	−2.40	0.001
MD	−2.67	0.030	−4.68	<0.001
MA	−2.46	0.001	−4.54	<0.001
MI	−1.79	<0.001	−2.86	<0.001
MN	−1.06	<0.001	−1.41	<0.001
MS	−1.49	<0.001	−1.32	0.118
MO	−2.00	<0.001	−2.85	<0.001
MT	−0.71	0.003	−0.80	<0.001
NE	−1.10	<0.001	−1.57	<0.001
NV	−0.85	<0.001	−0.90	0.001
NH	−2.38	<0.001	−4.18	<0.001
NJ	−2.51	0.002	−4.89	<0.001
NM	−0.85	<0.001	−0.75	0.022
NY	−2.25	<0.001	−4.03	<0.001
NC	−2.21	<0.001	−3.13	<0.001
ND	−0.72	0.008	−0.83	<0.001
OH	−2.72	<0.001	−4.63	<0.001
OK	−1.47	<0.001	−1.44	<0.001
OR	−0.68	0.045	−0.67	0.405
PA	−2.85	<0.001	−5.17	<0.001
RI	−2.39	0.019	−4.68	0.018
SC	−1.83	<0.001	−2.30	0.002
SD	−0.90	<0.001	−1.22	<0.001
TN	−2.40	<0.001	−3.21	<0.001
TX	−1.14	<0.001	−0.67	0.058
UT	−1.00	<0.001	−1.07	<0.001
VT	−2.04	<0.001	−3.51	<0.001
VA	−2.78	<0.001	−4.56	<0.001
WA	−0.67	0.075	−0.48	0.531
WV	−3.01	<0.001	−5.12	<0.001
WI	−1.50	<0.001	−2.23	<0.001
WY	−0.87	<0.001	−0.95	<0.001

the ORI_180s and the ORI_1800s appear, with the highest positive value 0.26 ppb and negative value −0.54 ppb. However, the Student's *t* test shown in Table 4 indicates that the difference of summertime mean surface ozone concentration between the ORI_180s and the ORI_1800s is again not statistically significant at $\alpha=0.05$. As stated before, the summertime mean surface ozone concentration is strongly overestimated by the current version of CAM4-Chem. By keeping the same first-order implicit solver but using the 180 s rather than 1800 s time step, the prediction bias seems to be reduced nationwide except at five states (Alabama: 0.16 ppb, Mississippi: 0.12 ppb, Georgia: 0.13 ppb, South Carolina: 0.04 ppb, and Louisiana: 0.16 ppb). Nevertheless, the benefit is less visible due to the small difference (difference of $E_{MNGE} < 1\%$ for most states) and neither the positive nor negative difference is statistically significant. Therefore, we cannot conclude that a better prediction is obtained by simply refining the time step size. On the other hand, the ROS-2_1800s does provide statistically significant reduction of both annual and summertime mean surface ozone concentration bias over most conterminous states, as described in the previous section. Furthermore, the magnitude of surface ozone concentration decrease is also much higher than that here. This reflects the fact that the improvement from the ROS-2_1800s may not follow its second-order accuracy as we supposed, but instead from its suitability for stiff problems [*Shampine*, 1982; *Verwer et al*., 1999]. Based on the results of numerical analysis in section 3.1, the first-order solver may converge to the "exact" solution at tiny time step size but the computation will be unaffordable in the real simulation of an earth system model. However, the ROS-2 solver is likely to converge to the "exact" solution with relatively large time step size and the ROS-2 solver with 1800 s time step has already provided a solution with small relative error. So we think the ROS-2_1800s solver could handle stiff system better than the original first-order implicit solver and thus provide a better estimate of surface ozone concentration, especially for the summer season.

3.4. ROS-2 Solver With 180 and 1800 s Time Step

As stated above, the ROS-2_1800s reduces the surface ozone concentration bias between simulation and observation data. A further question is raised: Can the ROS-2 solver benefit from refining the time step size?

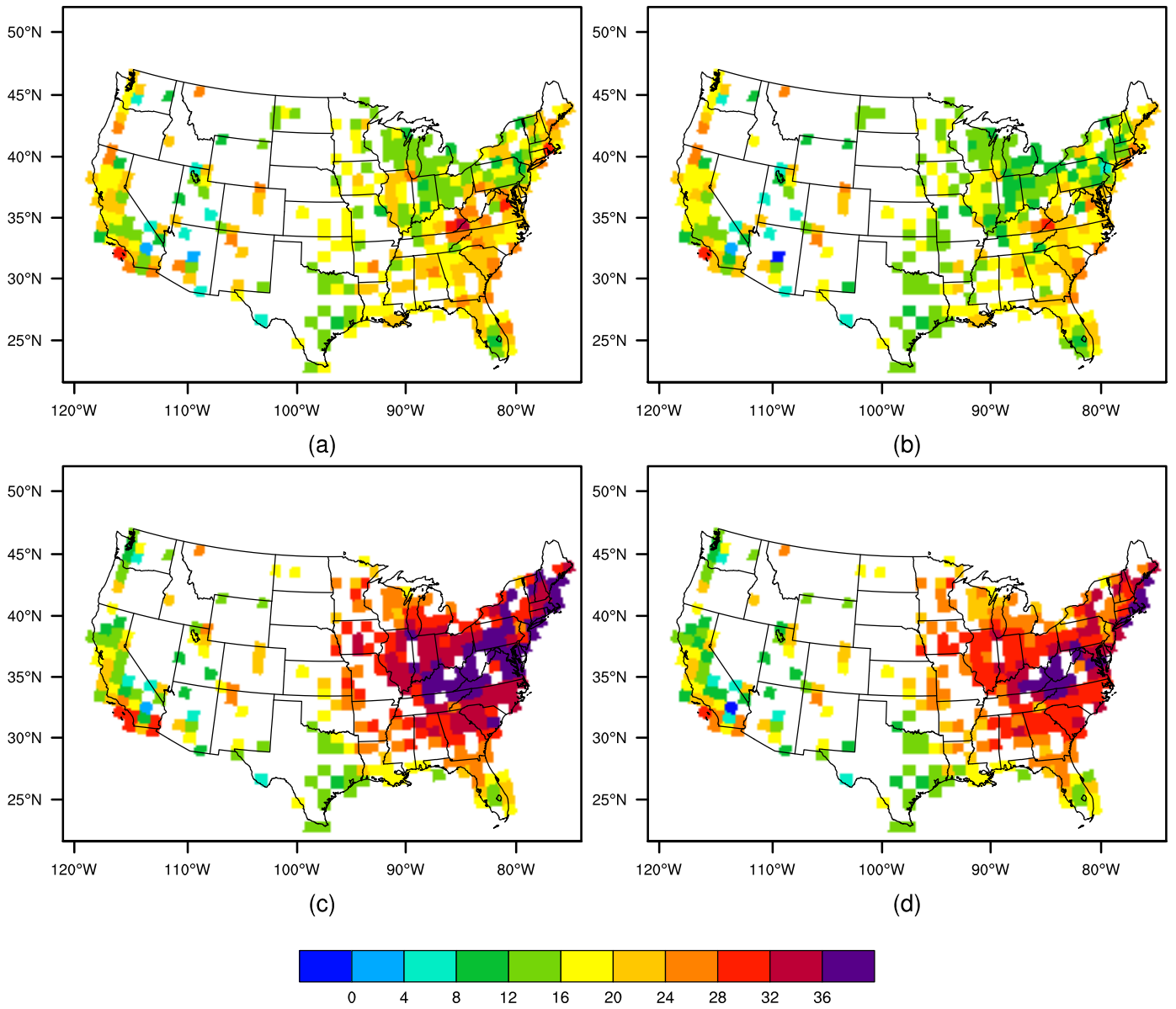

Figure 3. Ten year averaged (a) annual and (c) summertime mean surface ozone concentration bias (units: ppb) over the CONUS between the ORI_1800s and the AQS observation data (ORI_1800s minus AQS). (b, d) The same but for the ROS-2_1800s.

To answer this question, another time-slice simulation is conducted by using the ROS-2 solver with 180 s time step (ROS-2_180s). The difference of 10 year averaged annual mean surface ozone concentration between the ROS-2_180s and the ROS-2_1800s (ROS-2_180s minus ROS-2_1800s) is plotted in Figure 5a. Surprisingly, the ROS-2_180s provides a nationwide higher estimate of surface ozone concentration, ranging from 0.16 to 2.15 ppb. The primary difference is located in the Eastern U.S. with the largest and smallest state-level differences in West Virginia and New Mexico, respectively (see Table 5). The Student's *t* test suggests that the difference between the ROS-2_180s and the ROS-2_1800s is statistically significant over 32 states at $\alpha=0.05$, varying from 0.42 to 2.07 ppb. The difference of 10 year averaged summertime mean surface ozone concentration between the ROS-2_180s and the ROS-2_1800s is shown in Figure 5b. Instead of a consistently higher estimate of surface ozone concentration over the CONUS in Figure 5a, some slight decreases are observed at parts of Texas and New Mexico. It presents a wider range of difference at grid-cell level from −0.19 to 4 ppb. The state-level differences shown in Table 5 indicate that the ROS-2_180s still generates a higher estimate of summertime ozone concentration over most parts of the CONUS, similar to

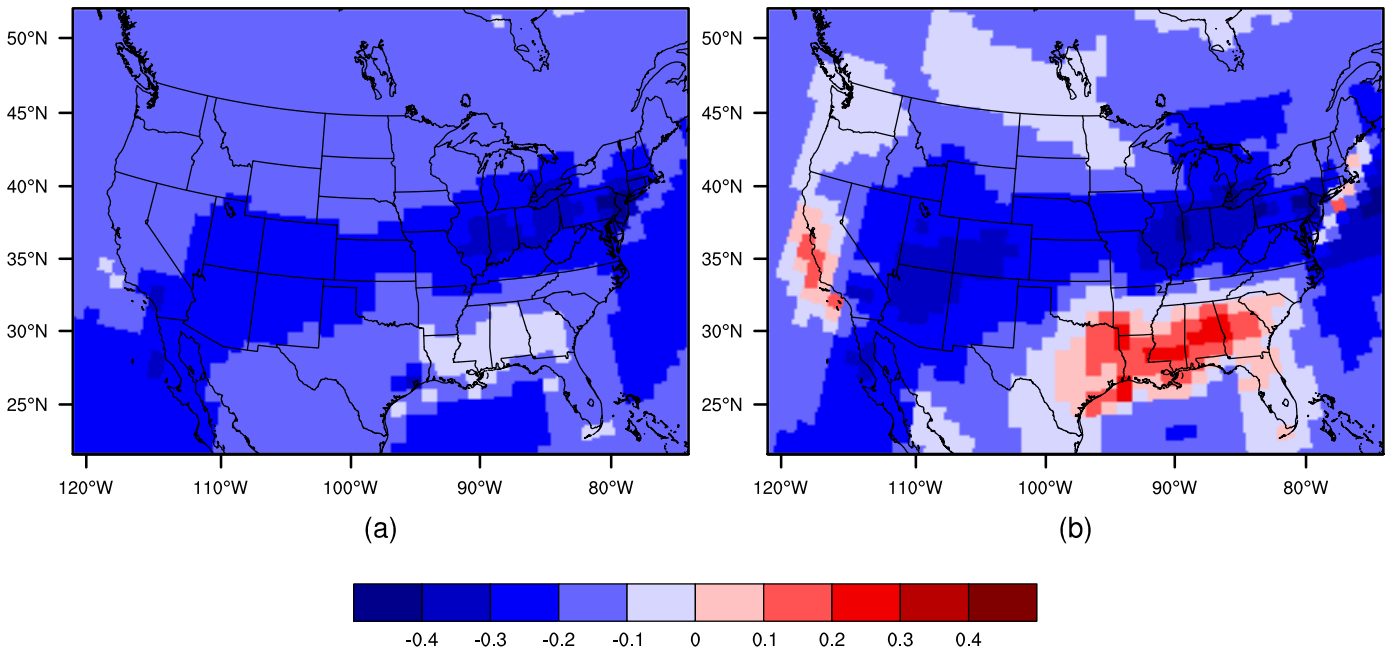

Figure 4. Difference of 10 year averaged (a) annual and (b) summertime mean surface ozone concentration (units: ppb) over the CONUS between the first-order implicit solver at 180 s time step (ORI_180s) and the ORI_1800s (ORI_180s minus ORI_1800s).

the results in Figure 5a. However, the Student's *t* test suggests that these differences are statistically significant over 28 states at α=0.05, varying from 0.41 to 3.71 ppb. As demonstrated in Figure 3, the ROS-2_1800s is still likely to overestimate the surface ozone concentration over the CONUS. Therefore, the ROS-2_180s seems to increase the surface ozone concentration bias and no benefit is obtained for the ROS-2 solver from refining the chemistry time step size in this case. However, compared to the ORI_180s and ORI_1800s (see Figures (2 and 4), and 5), the ROS-2_180s still reduces the surface ozone concentration bias to some extent (up to 2 ppb for summer season). Therefore, the ROS-2_180s at least does not negatively impact the chemistry calculation compared with the original first-order implicit solver. From section 3.1, both ROS-2_180s and ROS-2_1800s provide small relative errors and do not differ too much from each other (see Tables 1 and 2). Thus, we think some other factors may play a role here. We output the system matrices from the selected grid cells used in section 3.1 and calculate the condition numbers of the matrices using the function cond() in MATLAB. All of them are larger than 10^{12}, which means the system matrices are strongly ill-conditioned and a minor change of left-hand side system matrix or right-hand side vector could lead to a major difference in the final solution. For the box model, the solution of the current time step will be used as the input for the next time step integration. Nevertheless, in the real simulation of CAM4-Chem, other processes like advection and diffusion will bring some additional mass from the neighboring grid cells or transfer some mass from the current grid cell, leading to a "discontinuity" of the solution between the end of the current time step and the beginning of the next time step. The effect of "discontinuity" may be amplified by the ill-conditioned system and partially contributes to the difference between the ROS-2_180s and the ROS-2_1800s. It reminds us that the earth system model is very complex and the improvement from the ROS-2 solver may not be limited to its numerical properties, but also related to its interaction with other processes (e.g., dynamics) and components (e.g., land and ocean). The exact reason can only be explored by additional case studies but that is beyond the scope of this study.

3.5. Evaluation of Surface Ozone Concentration at Global Scale

Though this work mainly focuses on the bias of surface ozone concentration over the CONUS, model comparisons for variables at the global scale are necessary since CAM4-Chem is a global chemistry-climate model. The difference of 10 year averaged global surface ozone concentration between the ROS-2_1800s and the ORI_1800s is shown in Figure 6. The clear decrease of surface ozone concentration predicted by the ROS-2_1800s is observed for both annual mean (Figure 6a) and JJA mean (Figure 6b) results. In particular, greater than 3 ppb reduction occurs in Western Europe and Northeast China during the summer season.

Table 4. Statistics for the First-Order Implicit Solver at 180 s Time Step (ORI_180s) and 1800 s Time Step (ORI_1800s) in Each State, Respectively

					Mean Normalized Gross Error (%)			
					ORI_1800s		ORI_180s	
State	Annual Mean Bias	*p* Value	Summer Mean Bias	*p* Value	Annual	Summer	Annual	Summer
AL	−0.07	0.770	0.16	0.810	81.31	104.00	81.05	104.55
AZ	−0.24	0.246	−0.31	0.341	44.06	43.22	43.44	42.50
AR	−0.15	0.624	−0.03	0.942	64.43	81.66	63.95	81.63
CA	−0.18	0.549	−0.07	0.910	65.09	46.81	64.51	46.74
CO	−0.22	0.298	−0.30	0.053	57.51	49.84	56.89	49.13
CT	−0.33	0.673	−0.28	0.822	55.35	97.68	54.23	96.88
DE	−0.32	0.686	−0.29	0.769	88.26	104.58	87.03	103.77
FL	−0.14	0.758	0.00	0.999	67.31	86.78	66.81	86.76
GA	−0.09	0.770	0.13	0.881	78.54	102.13	78.22	102.61
ID	−0.15	0.591	−0.16	0.619	45.54	44.83	45.10	44.43
IL	−0.28	0.398	−0.33	0.259	70.47	96.98	69.44	95.99
IN	−0.33	0.397	−0.39	0.317	49.21	100.04	48.17	98.93
IA	−0.20	0.485	−0.24	0.477	67.42	98.33	66.70	97.55
KS	−0.21	0.402	−0.25	0.280	65.71	60.78	64.98	60.13
KY	−0.26	0.567	−0.23	0.615	76.22	120.02	75.34	119.31
LA	−0.09	0.826	0.16	0.843	76.44	84.65	76.10	85.23
ME	−0.18	0.637	−0.16	0.828	67.74	117.68	67.10	117.17
MD	−0.27	0.819	−0.24	0.838	88.58	116.22	87.62	115.56
MA	−0.27	0.698	−0.21	0.867	77.15	108.69	76.19	108.07
MI	−0.23	0.457	−0.26	0.667	51.34	86.75	50.58	85.92
MN	−0.14	0.564	−0.10	0.777	61.55	85.35	61.02	84.99
MS	−0.08	0.827	0.12	0.892	65.70	83.33	65.41	83.74
MO	−0.22	0.536	−0.25	0.488	59.57	84.60	58.85	83.98
MT	−0.15	0.533	−0.14	0.427	91.86	85.99	91.30	85.55
NE	−0.20	0.399	−0.25	0.154	38.78	42.86	38.27	42.32
NV	−0.18	0.406	−0.22	0.445	58.92	45.87	58.44	45.48
NH	−0.26	0.679	−0.20	0.851	74.45	126.73	73.48	126.05
NJ	−0.52	0.509	−0.52	0.660	46.58	84.76	44.66	83.25
NM	−0.21	0.372	−0.26	0.437	62.04	45.99	61.40	45.36
NY	−0.23	0.607	−0.21	0.713	65.25	109.30	64.47	108.64
NC	−0.18	0.529	−0.11	0.834	74.54	101.68	73.95	101.33
ND	−0.13	0.641	−0.09	0.684	52.50	57.42	52.07	57.10
OH	−0.31	0.281	−0.36	0.247	56.65	98.21	55.62	97.18
OK	−0.19	0.542	−0.11	0.778	50.69	48.86	50.11	48.63
OR	−0.13	0.703	−0.07	0.932	88.31	66.15	87.80	66.06
PA	−0.31	0.407	−0.30	0.462	66.68	108.20	65.58	107.30
RI	−0.23	0.811	−0.16	0.935	116.77	118.70	115.82	118.24
SC	−0.13	0.735	0.04	0.961	85.54	116.14	85.09	116.27
SD	−0.16	0.530	−0.17	0.437	43.84	41.09	43.34	40.59
TN	−0.18	0.552	−0.09	0.819	66.94	97.24	66.38	97.01
TX	−0.18	0.315	−0.05	0.889	52.15	51.04	51.51	51.16
UT	−0.22	0.358	−0.29	0.182	38.64	37.14	38.05	36.50
VT	−0.21	0.656	−0.15	0.855	43.96	78.53	43.32	78.10
VA	−0.24	0.490	−0.23	0.543	93.04	135.11	92.19	134.38
WA	−0.14	0.713	−0.04	0.954	96.26	63.51	95.53	63.29
WV	−0.27	0.565	−0.28	0.541	91.46	135.65	90.44	134.77
WI	−0.18	0.494	−0.16	0.675	50.81	82.15	50.25	81.67
WY	−0.18	0.444	−0.23	0.282	47.29	46.10	46.78	45.56

We further compare the model results to the observation data in Europe from the European Monitoring and Evaluation Program (EMEP, http://www.emep.int/) and Asia from the Acid Deposition Monitoring Network in East Asia (EANET, http://www.eanet.asia/). For Europe, the observed 10 year averaged annual mean ozone concentration is (mean ± standard deviation over space) 32.83 ± 8.12 ppb while those for the ORI_1800s and the ROS-2_1800s are 48.69 ± 7.83 and 47.32 ± 7.76 ppb, respectively. Considering the 10 year averaged JJA mean ozone concentration, the observation value is 37.21 ± 10.08 ppb while those for the ORI_1800s and the ROS-2_1800s are 57.74 ± 12.27 and 55.65 ± 11.76 ppb, respectively. For Asia, the observed 10 year averaged annual mean ozone concentration is 34.06 ± 11.51 ppb while the values from the ORI_1800s and the ROS-2_1800s are 44.91 ± 5.39 and 43.99 ± 5.17 ppb, respectively. For the 10 year averaged JJA mean ozone concentration, the observed value is 27.91 ± 12.43 ppb while the values from the

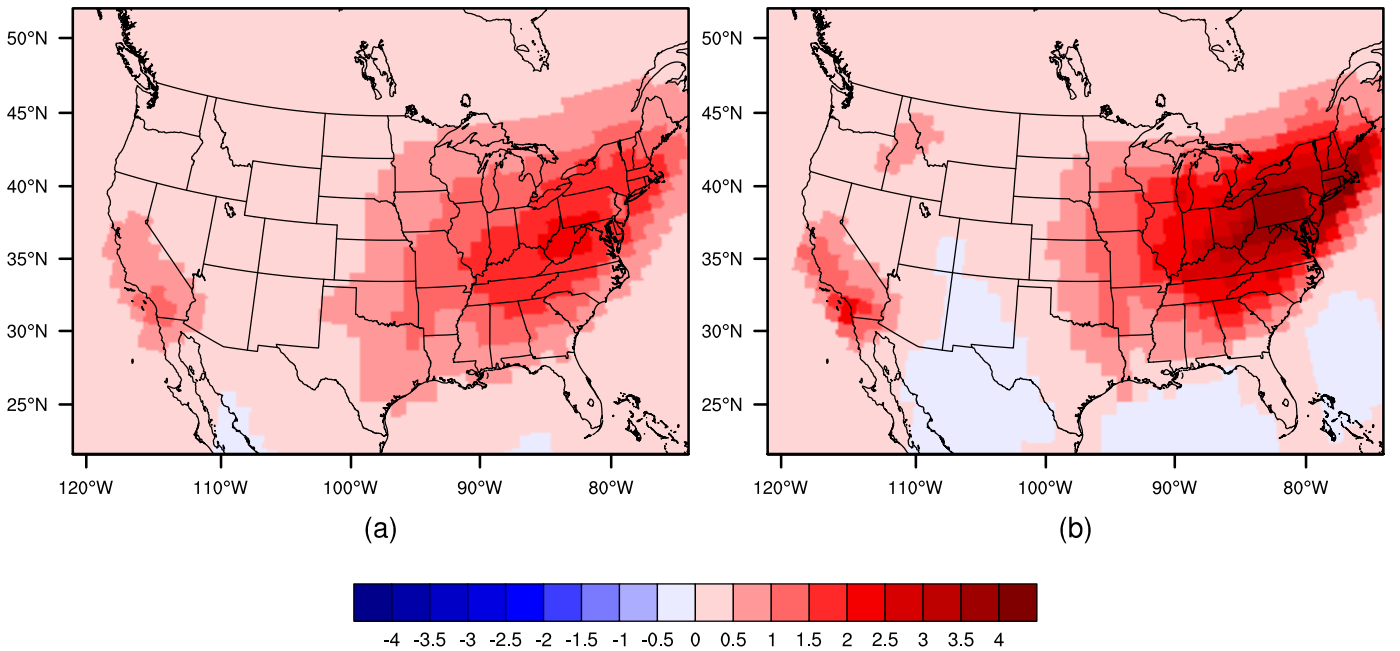

Figure 5. Difference of 10 year averaged (a) annual and (b) summertime mean surface ozone concentration (units: ppb) over the CONUS between the ROS-2 solver at 180 s time step (ROS-2_180s) and the ROS-2_1800s (ROS-2_180s minus ROS-2_1800s).

ORI_1800s and the ROS-2_1800s are 37.43 ± 11.01 and 36.55 ± 10.57 ppb, respectively. Similar to the U.S., both solvers overestimate the surface ozone concentration over the European and Asian continents, especially for the JJA season. However, the comparison between model simulation results and observation data suggests that the ROS-2_1800s is able to reduce the bias more at the European sites. One main reason is that most of the Asian observation stations are in Japan, Korea, and Thailand, where less difference is seen from Figure 6. It is also worth noting that the observed JJA mean ozone concentration is lower than the annual mean value. This can be explained by the fact that more than half of the available ozone observation data come from sites in Japan and the concentrations there are highest in spring but lowest in summer at all stations [*Chatani and Sudo*, 2011; *Li et al*., 2016]. This comparison reveals that the ozone concentration is globally decreased by the ROS-2_1800s instead of a random fluctuation. Therefore, the lower surface ozone concentration over the CONUS predicted by the ROS-2_1800s is not a trade-off against increasing the surface ozone concentration in other global regions.

3.6. Computational Efficiency

Since the ROS-2 solver utilizes the same Jacobian matrix and LU factorization structure between the two stages, it is expected to speed up the computation compared to the original first-order implicit solver. Using the default simulation period setting (5 days), Table 6 summarizes the global statistics of average computational time per processor as a function of different numbers of threads. The percent of saved computational time and the factor of speedup are calculated by the following equations:

$$\text{Time per processor} = \frac{\text{Total time}}{\text{NTASKS\_ATM} * \text{NTHRDS\_ATM}} \tag{7}$$

$$\text{Percent of saved time} = \frac{T_{ORI} - T_{ROS-2}}{T_{ORI}} \tag{8}$$

$$\text{Factor of speedup} = \frac{T_{ORI}}{T_{ROS-2}} \tag{9}$$

where "Total time" means the total summed wall-clock time consumed over all the processors. "NTASKS_ATM" and "NTHRDS_ATM" are variables that set the number of MPI tasks and the number of OpenMP threads per task, respectively. The product of these two variables specifies the total computational processors for the atmospheric component of CESM. T_{ORI} and T_{ROS-2} refer to the computational time of the first-order implicit

Table 5. Statistics for the Second-Order Rosenbrock Solver at 180 s Time Step (ROS-2_180s) and 1800 s Time Step (ROS-2_1800s) in Each State, Respectively

					Mean Normalized Gross Error (%)			
					ROS-2_1800s		ROS-2_180s	
State	Annual Mean Bias	*p* Value	Summer Mean Bias	*p* Value	Annual	Summer	Annual	Summer
AL	1.11	<0.001	1.02	0.102	74.69	97.49	79.02	101.39
AZ	0.42	0.039	0.34	0.272	41.12	39.86	42.30	40.91
AR	1.06	<0.001	1.02	0.001	58.72	75.94	62.16	78.99
CA	0.69	0.019	0.82	0.189	61.11	43.47	63.44	45.80
CO	0.39	0.064	0.14	0.377	54.71	47.23	55.83	47.59
CT	1.77	0.026	3.50	0.004	46.39	83.66	52.34	93.79
DE	1.74	0.035	3.24	0.003	78.10	91.86	84.72	100.76
FL	0.44	0.312	0.14	0.850	63.72	84.24	65.26	84.80
GA	1.06	<0.001	1.12	0.182	72.31	95.82	76.32	99.83
ID	0.38	0.173	0.42	0.177	43.39	42.63	44.48	43.65
IL	1.36	<0.001	1.94	<0.001	62.14	86.09	67.02	91.96
IN	1.57	<0.001	2.42	<0.001	40.81	87.68	45.93	94.86
IA	0.90	0.001	1.23	<0.001	61.69	90.25	64.88	94.19
KS	0.61	0.016	0.59	0.007	60.76	55.57	63.28	57.69
KY	1.84	<0.001	2.71	<0.001	66.61	107.21	72.98	115.42
LA	0.74	0.062	0.47	0.538	71.82	82.01	74.50	83.62
ME	1.00	0.007	1.68	0.018	61.72	107.22	65.89	114.97
MD	1.81	0.134	3.34	0.006	79.03	103.12	85.52	112.49
MA	1.69	0.016	3.39	0.005	68.28	95.03	74.37	105.24
MI	1.11	<0.001	1.72	0.002	45.19	77.31	49.03	83.09
MN	0.57	0.018	0.67	0.044	57.37	79.85	59.70	82.64
MS	0.89	0.012	0.63	0.439	60.63	79.00	63.63	81.06
MO	1.15	0.001	1.36	<0.001	53.11	76.74	56.82	80.61
MT	0.34	0.152	0.32	0.064	89.13	83.27	90.51	84.60
NE	0.50	0.032	0.52	0.002	36.21	40.13	37.29	40.74
NV	0.39	0.060	0.26	0.354	56.16	43.42	57.54	44.41
NH	1.66	0.011	3.14	0.002	65.65	112.08	71.78	123.12
NJ	1.32	0.085	3.02	0.012	37.26	70.68	42.18	79.40
NM	0.28	0.237	−0.05	0.881	59.49	44.28	60.28	44.02
NY	1.58	0.001	3.00	<0.001	57.52	96.48	62.96	106.03
NC	1.46	<0.001	2.01	<0.001	67.22	92.39	72.10	98.39
ND	0.33	0.213	0.29	0.182	50.20	55.01	51.22	55.76
OH	1.77	<0.001	3.02	<0.001	47.72	85.08	53.52	93.62
OK	0.80	0.008	0.65	0.084	45.85	44.93	48.57	46.82
OR	0.37	0.279	0.39	0.622	85.48	63.72	87.04	65.35
PA	1.93	<0.001	3.71	<0.001	56.79	93.03	63.48	103.91
RI	1.65	0.089	3.53	0.062	106.95	105.15	113.74	115.37
SC	1.18	0.001	1.46	0.042	79.02	108.52	83.21	113.33
SD	0.41	0.099	0.41	0.046	41.42	38.59	42.39	39.09
TN	1.59	<0.001	1.95	<0.001	59.23	87.88	64.38	93.73
TX	0.57	0.002	0.24	0.484	47.54	48.86	50.07	50.08
UT	0.40	0.098	0.14	0.522	35.92	34.69	37.01	35.04
VT	1.44	0.002	2.65	0.001	37.76	68.61	42.13	76.09
VA	1.93	<0.001	3.19	<0.001	83.14	120.85	90.00	130.78
WA	0.35	0.352	0.28	0.712	92.88	61.39	94.63	62.61
WV	2.07	<0.001	3.58	<0.001	80.47	119.75	88.00	130.81
WI	0.91	<0.001	1.28	<0.001	46.08	75.47	48.94	79.29
WY	0.38	0.114	0.19	0.373	44.83	43.83	45.89	44.27

solver and the ROS-2 solver with given number of processors, respectively. The Titan supercomputer at Oak Ridge National Laboratory (ORNL) is used for performance testing. Titan is a hybrid-architecture Cray XK7 system with 18,688 compute nodes (16 processors per node) and a theoretical peak performance exceeding 27 petaflops. The chemistry update takes the longest time per processor when only 48 processors are requested, but it drops rapidly as the number of processors increases (see Table 6). The average speedup of computational time for the ROS-2_1800s over that for ORI_1800s is around 1.95 when the total requested processors are less than or equal to 768 but reduces slightly to 1.83 when more processors are used. Similarly, the average speedup of computational time for the ROS-2_180s over that for the ORI_180s is about 1.88 when the total requested processors are less than or equal to 768 but reduces slightly to 1.77 with more processors. For the first-order implicit solver, using one tenth of the time step size does not simply result to

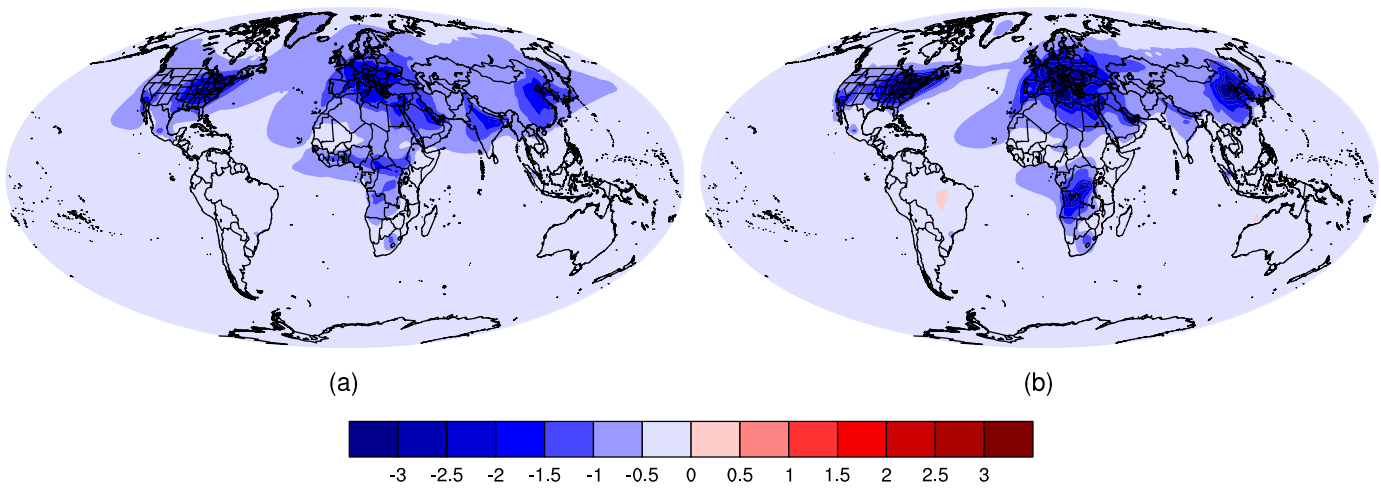

Figure 6. Difference of 10 year averaged (a) annual and (b) JJA mean surface ozone concentration (units: ppb) between the ROS-2_1800s and the ORI_1800s (ROS-2_1800s minus ORI_1800s) over the global continents.

a slower performance by a factor of 10. This is probably due to the fact that with a finer time step, fewer iteration steps are required for the chemistry solver to converge. For the ROS-2 solver, it is similarly found that the ROS-2_180s is not 10 times slower than then ROS-2_1800s. This is mainly caused by the adaptive time step method implemented in the ROS-2_1800s, which introduces additional computation at refined time step level and impedes the performance. Generally, the computational time per processor for the ROS-2_1800s is about 48% less than that for ORI_1800s and the computational time per processor for the ROS-2_180s is about 46% less than that for the ORI_180s. The ORI_1800s and ROS-2_1800s are further used to conduct 1 month and 1 year simulations separately to examine whether more improvements are possible (see Table 6). By requesting 1536 processors, the ROS-2_1800s takes about 47% less computational time than ORI_1800s for both 1 month and 1 year simulations, indicating that the performance improvement of the ROS-2_1800s over the ORI_1800s is stable at around 47%, regardless of the simulation period. It is worth noting that we use the same routines to form the Jacobian matrix and conduct the LU factorization for both solvers, which makes the comparison of performance fair. Therefore, the faster computational speed of the ROS-2 solver should be attributed to the advantage of numerical algorithm itself that avoids the reevaluation of Jacobian matrix and LU factorization between two stages.

Table 6. Summary of Computational Time (Units: s) per Processor for Each Solver (ORI_180s, ORI_1800s, ROS-2_180s, and ROS-2_1800s) With Various Simulation Periods

Simulation Period	Number of Processors	Computational Time per Processor for Each Solver			
		ORI_1800s	ROS-2_1800s	Percent of Saved Time	Speedup
5 days	48	714	370	48.18	1.93
	96	359	185	48.47	1.94
	192	180	93	48.33	1.94
	384	91	47	48.35	1.94
	768	46	23	50.00	2.00
	1536	22	12	45.45	1.83
	3072	11	6	45.45	1.83
5 days		ORI_180s	ROS-2_180s	Percent of Saved Time	Speedup
	48	5133	2,724	46.93	1.88
	96	2568	1,363	46.92	1.88
	192	1287	681	47.09	1.89
	384	645	340	47.29	1.90
	768	310	167	46.13	1.86
	1536	145	82	43.45	1.77
	3072	72	41	43.06	1.76
		ORI_1800s	ROS-2_1800s	Percent of Saved Time	Speedup
1 month	1536	139	73	47.48	1.90
		ORI_1800s	ROS-2_1800s	Percent of Saved Time	Speedup
1 year	1536	1607	844	47.48	1.90

4. Conclusion

To the authors' knowledge, this is the first study of implementing the ROS-2 solver in CAM4-Chem and evaluating its impact on the prediction of surface ozone concentration over the CONUS. Compared to the ORI_1800s, the ROS-2_1800s is likely to provide consistently nationwide lower 10 year averaged annual mean surface ozone concentration (see Figure 2a) and the Student's *t* test suggests that the difference is statistically significant over 47 states at α=0.05. For the summertime, the ROS-2_1800s similarly presents a significantly lower estimate of 10 year averaged surface ozone concentration over the CONUS. The absolute difference is much larger (up to 5.2 ppb for one state) and 42 out of 48 states are statistically significant at α=0.05. This implies that the ROS-2_1800s can help improve the performance of surface ozone concentration over the CONUS, especially during the summer season when the photochemical reactions are the most active. The lower global surface ozone concentration generated by the ROS-2_1800s also suggests that its prediction of lower surface ozone concentration over the CONUS is not a random fluctuation and the model evaluation shows that the ROS-2_1800s can reduce the bias in Europe and Asia to some extent as well.

In addition, the time step size for the original first-order implicit solver is refined to 180 s (one tenth of the default time step) to examine whether it could help improve the estimate of surface ozone concentration over the CONUS. Figure 4 shows that compared to ORI_1800s, ORI-180s does slightly reduce the surface ozone concentration but the improvement is less visible (only around 0.5 ppb as maximum) and not statistically significant, either. This reveals that just refining the time step size by a factor of 10 for the original first-order implicit solver is not able to provide statistically significant improvement of surface ozone concentration prediction. Thus, it is necessary to use other chemical solvers like the ROS-2 solver in this study. However, the outperformance for the ROS-2 solver may not come from its second-order accuracy with respect to time scale, but from its suitability for solving stiff problems. We have also applied the 180 s time step to the ROS-2 solver but the ROS-2_180s surprisingly performs worse than the ROS-2_1800s for estimating the surface ozone concentration. By studying some selected grid cells, the system matrix is found to be strongly ill-conditioned and other processes (e.g., diffusion) will cause "discontinuity" for the solution between the end of the current time step and the beginning of the next time step. The ROS-2 solvers with different time step sizes could converge to different solutions after a long-term simulation. In the real application, the CAM4-Chem may accumulate errors from other processes like dynamics and physics. Thus, the time step size for the ROS-2 solver in chemistry should be chosen carefully in order to provide a compensation of error.

The computational efficiencies of the ORI_1800s, ORI_180s, ROS-2_1800s and ROS-2_180s are also analyzed. Even if the first-order implicit solver has been optimized to solve the chemical reaction system efficiently, the ROS-2 solver takes about 47% less computational time than the original first-order implicit solver when using the same time step size. Our analysis indicates this speedup is explained by the fact that the ROS-2 solver utilizes the same Jacobian matrix and LU factorization structure during the two-stage calculations, which could consume 90% of the total computational time for the chemistry update. It is also observed that the ROS-2_180s is not 10 times slower than the ROS-2_1800s because of the adaptive time step method implemented in the ROS-2_1800s.

In future work, case studies with different configurations may be explored to examine whether the benefit of the ROS-2 solver observed in this study still persists. Other solvers from the Rosenbrock family (e.g., ROS-3) can also be implemented to see whether further bias reduction is possible for the surface ozone concentration prediction over the CONUS. Since all the constituents except water vapor are treated as radiatively inactive by default, the reduction of ozone concentration from the ROS-2_1800s is not expected to influence the longwave and shortwave cloud forcings in the current simulation but it is worth investigating the differences in a fully interactive simulation in future work. The chemistry update behaves like a box model in CAM4-Chem, which is an ideal target for parallel implementations. Either NVIDIA CUDA or OpenACC could be used as a programming model on advanced high performance computing platforms to harness the power of the GPU and further improve the computational performance.

Acknowledgments
This research is supported by the university subproject of the DOE SciDAC project "Chemistry in CESM-SE: Evaluation, Performance and Optimization" (UCAR subaward Z12-93537 to University of Tennessee - Knoxville). The production run uses the resources of the Oak Ridge Leadership Computing Facility at the Oak Ridge National Laboratory, which is supported by the Office of Science of the U.S. Department of Energy (contract DE-AC05-00OR22725). The diagnostic simulation and analysis of numerical convergence rate use the computing resources (ark:/85065/d7wd3xhc) provided by the Climate Simulation Laboratory at NCAR's Computational and Information Systems Laboratory, sponsored by the National Science Foundation and other agencies. The CESM project is supported by the National Science Foundation and the Office of Science (BER) of the U.S. Department of Energy. The authors want to thank Patrick H. Worley at ORNL to help characterize and monitor the computational performance. NCAR is sponsored by the National Science Foundation. The source code for the model used in this study, the CAM4-Chem, is freely available at http://www.cesm.ucar.edu/models/cesm1.2/. The ozone observation data used to generate figures and tables for United States, Europe, and Asia in this study are archived at AQS (https://www.epa.gov/aqs), EMEP (http://www.emep.int/), and EANET (http://www.eanet.asia/). The model output data are available from the authors upon request (jsfu@utk.edu).

References

Blom, J. G., and J. G. Verwer (2000), A comparison of integration methods for atmospheric transport-chemistry problems, *J. Comput. Appl. Math.*, *126*, 381–396, doi:10.1016/S0377-0427(99)00366-0.

Chatani, S., and K. Sudo (2011), Influences of the variation in inflow to East Asia on surface ozone over Japan during 1996–2005, *Atmos. Chem. Phys.*, *11*, 8745–8758, doi:10.5194/acp-11-8745-2011.
Cooper, O. R., et al. (2010), Increasing springtime ozone mixing ratios in the free troposphere over western North America, *Nature*, *463*, 344–348, doi:10.1038/nature08708.
Daescu, D., G. R. Carmichael, and A. Sandu (2000), Adjoint implementation of Rosenbrock methods applied to variational data assimilation problems, *J. Comput. Phys.*, *165*, 496–510, doi:10.1006/jcph.2000.6622.
Emmons, L. K., et al. (2010), Description and evaluation of the Model for Ozone and Related chemical Tracers, version 4 (MOZART-4), *Geosci. Model Dev.*, *3*, 43–67, doi:10.5194/gmd-3-43-2010.
Fiore, A. M., et al. (2009), Multimodel estimates of intercontinental source-receptor relationships for ozone pollution, *J. Geophys. Res.*, *114*, D04301, doi:10.1029/2008JD010816.
Fiore, A. M., J. T. Oberman, M. Y. Lin, L. Zhang, O. E. Clifton, D. J. Jacob, V. Naik, L. W. Horowitz, J. P. Pinto, and G. P. Milly (2014), Estimating North American background ozone in U.S. surface air with two independent global models: Variability, uncertainties, and recommendations, *Atmos. Environ.*, *96*, 284–300, doi:10.1016/j.atmosenv.2014.07.045.
Fiscus, E. L., F. L. Booker, and K. O. Burkey (2005), Crop responses to ozone: Uptake, modes of action, carbon assimilation and partitioning, *Plant Cell Environ.*, *28*, 997–1011, doi:10.1111/j.1365-3040.2005.01349.x.
Hollaway, M. J., S. R. Arnold, A. J. Challinor, and L. D. Emberson (2012), Intercontinental trans-boundary contributions to ozone-induced crop yield losses in the Northern Hemisphere, *Biogeosciences*, *9*(1), 271–292, doi:10.5194/bg-9-271-2012.
Jacobson, M. Z., and D. L. Ginnebaugh (2010), Global-through-urban nested three-dimensional simulation of air pollution with a 13,600-reaction photochemical mechanism, *J. Geophys. Res.*, *115*, D14304, doi:10.1029/2009JD013289.
Jacobson, M. Z., and R. P. Turco (1994), SMVGEAR: A sparse-matrix, vectorized gear code for atmospheric models, *Atmos. Environ.*, *28*(2), 273–284, doi:10.1016/1352-2310(94)90102-3.
Jacobson, M. Z., M. A. Delucchi, M. A. Cameron, and B. A. Frew (2015), Low-cost solution to the grid reliability problem with 100% penetration of intermittent wind, water, and solar for all purposes, *Proc. Natl. Acad. Sci. U. S. A.*, *112*(49), 15,060–15,065, doi:10.1073/pnas.1510028112.
Karnosky, D. F., J. M. Skelly, K. E. Percy, and A. H. Chappelka (2007), Perspectives regarding 50 years of research on effects of tropospheric ozone air pollution on US forests, *Environ. Pollut.*, *147*(3), 489–506, doi:10.1016/j.envpol.2006.08.043.
Kinnison, D. E., et al. (2007), Sensitivity of chemical tracers to meteorological parameters in the MOZART-3 chemical transport model, *J. Geophys. Res.*, *112*, D20302, doi:10.1029/2006JD007879.
Lamarque, J.-F., et al. (2012), CAM-Chem: Description and evaluation of interactive atmospheric chemistry in the Community Earth System Model, *Geosci. Model Dev.*, *5*, 369–411, doi:10.5194/gmd-5-369-2012.
Lapina, K., D. K. Henze, J. B. Milford, M. Huang, M. Y. Lin, A. M. Fiore, G. Carmichael, G. G. Pfister, and K. Bowman (2014), Assessment of source contributions to seasonal vegetative exposure to ozone in the U.S., *J. Geophys. Res. Atmos.*, *119*, 324–340, doi:10.1002/2013JD020905.
Lee, I. (2010), A robust ILU preconditioner using constraints diagonal Markowitz, ACM SE'10 Proceedings of the 48th Annual Southeast Regional Conference, vol. 15, pp. 1–6, ACM, New York, N. Y., doi: 10.1145/1900008.1900031.
Li, J., W. Y. Yang, Z. F. Wang, H. S. Chen, B. Hu, J. J. Li, Y. L. Sun, P. Q. Fu, and Y. Q. Zhang (2016), Modeling study of surface ozone source-receptor relationships in East Asia, *Atmos. Res.*, *167*, 77–88, doi:10.1016/j.atmosres.2015.07.010.
Linford, J. C., J. Michalakes, M. Vachharajani, and A. Sandu (2009), Multi-core acceleration of chemical kinetics for simulation and prediction, in *Proceedings of the Conference on High Performance Computing Networking, Storage and Analysis, SC '09*, vol. *7*, pp. 1–11, Assoc. for Comput. Mach., New York, doi:10.1145/1654059.1654067.
Long, M. S., W. C. Keene, R. Easter, R. Sander, A. Kerkweg, D. Erickson, X. Liu, and S. Ghan (2013), Implementation of the chemistry module MECCA (v2.5) in the modal aerosol version of the Community Atmosphere Model component (v3.6.33) of the Community Earth System Model, *Geosci. Model Dev.*, *6*, 255–262, doi:10.5194/gmd-6-255-2013.
Murazaki, K., and P. Hess (2006), How does climate change contribute to surface ozone change over the United States?, *J. Geophys. Res.*, *111*, D05301, doi:10.1029/2005JD005873.
Neale, R. B., et al. (2010), Description of the Community Atmosphere Model (CAM 4.0), NCAR Tech. Note TN-485+STR, 212 pp., National Center for Atmospheric Research, Boulder, Colo.
Neale, R. B., J. Richter, S. Park, P. H. Lauritzen, S. J. Vavrus, P. J. Rasch, and M. H. Zhang (2013), The Mean Climate of the Community Atmosphere Model (CAM4) in forced SST and fully coupled experiments, *J. Clim.*, *26*, 5150–5168, doi:10.1175/JCLI-D-12-00236.1.
Reidmiller, D. R., et al. (2009), The influence of foreign vs. North American emissions on surface ozone in the US, *Atmos. Chem. Phys.*, *9*, 5027–5042, doi:10.5194/acp-9-5027-2009.
Rotman, D. A., et al. (2001), Global Modeling Initiative assessment model: Model description, integration, and testing of the transport shell, *J. Geophys. Res.*, *106*(D2), 1669–1691, doi:10.1029/2000JD900463.
Rotman, D. A., et al. (2004), IMPACT, the LLNL 3-D global atmospheric chemical transport model for the combined troposphere and stratosphere: Model description and analysis of ozone and other trace gases, *J. Geophys. Res.*, *109*, D04303, doi:10.1029/2002JD003155.
Sandu, A., and R. Sander (2006), Technical note: Simulating chemical systems in Fortran90 and Matlab with the Kinetic PreProcessor KPP-2.1, *Atmos. Chem. Phys.*, *6*(1), 187–195, doi:10.5194/acp-6-187-2006.
Sandu, A., J. G. Verwer, M. Van Loon, G. R. Carmichael, F. A. Potra, D. Dabdub, and J. H. Seinfeld (1997), Benchmarking stiff ode solvers for atmospheric chemistry problems-I. Implicit vs explicit, *Atmos. Environ.*, *31*(19), 3151–3166, doi:10.1016/S1352-2310(97)00059-9.
Sarwar, G., J. Godowitch, B. H. Henderson, K. Fahey, G. Pouliot, W. T. Hutzell, R. Mathur, D. Kang, W. S. Goliff, and W. R. Stockwell (2013), A comparison of atmospheric composition using the Carbon Bond and Regional Atmospheric Chemistry Mechanisms, *Atmos. Chem. Phys.*, *13*, 9695–9712, doi:10.5194/acp-13-9695-2013.
Shampine, L. F. (1982), Implementation of Rosenbrock Methods, *Trans. Math. Software*, *8*(2), 93–113, doi:10.1145/355993.355994.
Stevenson, D. S., C. E. Johnson, W. J. Collins, R. G. Derwent, K. P. Shine, and J. M. Edwards (1998), Evolution of tropospheric ozone radiative forcing, *Geophys. Res. Lett.*, *25*(20), 3819–3822, doi:10.1029/1998GL900037.
Stevenson, D. S., et al. (2006), Multimodel ensemble simulations of present-day and near-future tropospheric ozone, *J. Geophys. Res.*, *111*, D08301, doi:10.1029/2005JD006338.
Stevenson, D. S., et al. (2013), Tropospheric ozone changes, radiative forcing and attribution to emissions in the Atmospheric Chemistry and Climate Model Intercomparison Project (ACCMIP), *Atmos. Chem. Phys.*, *13*, 3063–3085, doi:10.5194/acp-13-3063-2013.
Sun, J., J. S. Fu, K. Huang, and Y. Gao (2015), Estimation of future $PM_{2.5}$- and ozone-related mortality over the continental United States in a changing climate: An application of high-resolution dynamical downscaling technique, *J. Air Waste Manage. Assoc.*, *65*(5), 611–623, doi:10.1080/10962247.2015.1033068.

Val Martin, M., C. L. Heald, and S. R. Arnold (2014), Coupling dry deposition to vegetation phenology in the Community Earth System Model: Implications for the simulation of surface O3, *Geophys. Res. Lett.*, *41*, 2988–2996, doi:10.1002/2014GL059651.

Val Martin, M., C. L. Heald, J.-F. Lamarque, S. Tilmes, L. K. Emmons, and B. A. Schichtel (2015), How emissions, climate, and land use change will impact mid-century air quality over the United States: A focus on effects at national parks, *Atmos. Chem. Phys.*, *15*, 2805–2823, doi:10.5194/acp-15-2805-2015.

Verwer, J. G., E. J. Spee, J. G. Blom, and W. Hundsdorfer (1999), A second-order Rosenbrock method applied to photochemical dispersion problems, *SIAM J. Sci. Comput.*, *20*(4), 1456–1480, doi:10.1137/S1064827597326651.

Young, P. J., et al. (2013), Pre-industrial to end 21st century projections of tropospheric ozone from the Atmospheric Chemistry and Climate Model Intercomparison Project (ACCMIP), *Atmos. Chem. Phys.*, *13*, 2063–2090, doi:10.5194/acp-13-2063-2013.

Zeng, G., J. A. Pyle, and P. J. Young (2008), Impact of climate change on tropospheric ozone and its global budgets, *Atmos. Chem. Phys.*, *8*, 369–387, doi:10.5194/acp-8-369-2008.

Zhang, H., J. C. Linford, A. Sandu, and R. Sander (2011), Chemical Mechanism Solvers in Air Quality models, *Atmosphere*, *2*(3), 510–532, doi:10.3390/atmos2030510.